Ogawa et al. International Journal of Mechanical and Materials Engineering (2015) 10:12
DOI 10.1186/s40712-015-0044-9

International Journal of Mechanical and Materials Engineering
a SpringerOpen Journal

ORIGINAL ARTICLE Open Access

Hydrogen embrittlement behavior of Ni-Ti shape memory alloy with different microstructures in acidic fluoride solution

Toshio Ogawa[1*], Eishu Yokozawa[2], Tetsuro Oda[3], Kuniaki Maruoka[1] and Jun'ichi Sakai[3,4]

Abstract

Background: It is important to investigate the mechanism for the hydrogen embrittlement of Ni-Ti alloys in acidic fluoride solutions to improve the reliability and safety of these alloys as dental devices. Therefore, the hydrogen embrittlement behavior of Ni-Ti shape memory alloy immersed in acidic fluoride solution was investigated with a focus on the constituent phase in the microstructure of the alloy in this study.

Methods: Three microstructures with different phases (parent single phase, mixture of parent and martensite phases, and martensite single phase) were prepared by tensile loading and unloading. The specimens were immersed separately in 50 mL of 0.2 % acidulated phosphate fluoride (APF) solution with pH 5.0 at room temperature (25 °C) for various periods.

Results: After immersion for 2 h, the tensile strengths of all the specimens were not significantly changed with respect to those of the non-immersed specimens. After immersion for 4 h, the tensile strengths of all the specimens immersed were decreased with respect to those of the non-immersed specimens, and the tensile strength of the martensite single phase specimen (C) was higher than that of parent single phase specimen (A) and the parent/martensite mixed phase specimen (B). After immersion for 6 h, the tensile strengths of all the specimens were decreased with respect to those of the specimens immersed for 4 h, and the tensile strength of specimen B was lower than that of specimens A and C.

Conclusions: The susceptibility to hydrogen embrittlement of the Ni-Ti shape memory alloy with a microstructure including the parent phase tends to be high when the degree of corrosion is not significantly different for the alloy microstructure. Moreover, the effect of corrosion on the tensile strength of Ni-Ti shape memory alloy is significant when the microstructure includes the martensite phase. Hence, the significant degradation of tensile strength observed for specimen B was probably caused by a synergistic effect of hydrogen absorption and corrosion.

Keywords: Ni-Ti; Hydrogen embrittlement; Microstructure; Fluoride

Background

Ni-Ti alloys have been used widely as biomedical materials because they exhibit good corrosion resistance, excellent mechanical properties, and biocompatibility (Oshida et al. 1990; Shabalovskaya 2001; Lekston et al. 2004; Rondelli 1996; Rondelli and Vicentini 1999). However, the corrosion resistance of Ni-Ti alloys is not always satisfactory in the oral cavity (Yokoyama et al. 2001, 2004a; Cheng et al. 2003; Huang et al. 2003; Wang et al. 2007). It has been reported that the corrosion resistance of Ni-Ti alloys is lost in the oral cavity due to the presence of fluoride, which is contained in oral products such as toothpastes and prophylactic agents (Schiff et al. 2002, 2004; Li et al. 2007; Huang 2007; Lee et al. 2009; Mirjalili et al. 2013). Furthermore, Ni-Ti alloys absorb a substantial amount of hydrogen from acidic fluoride solutions, thereby causing hydrogen embrittlement of the alloys (Yokoyama et al. 2003a,

* Correspondence: ogawa@m.kisarazu.ac.jp
[1]Department of Mechanical Engineering, National Institute of Technology, Kisarazu College, 2-11-1 Kiyomidai-higashi, Kisarazu-shi, Chiba 292-0041, Japan
Full list of author information is available at the end of the article

2004b, 2005a). Accordingly, it is important to investigate the mechanism for the hydrogen embrittlement of Ni-Ti alloys in acidic fluoride solutions to improve the reliability and safety of these alloys as dental devices.

It is well known that the hydrogen embrittlement of metals is closely related to the microstructure of the metals (Takai and Watanuki 2003; Zhao et al. 2014; Nakasato and Terasaki 1975; Gu et al. 2002; Nozue et al. 1987, 1998; Yokoyama et al. 2003b, 2004c, d, 2005b, 2009; Kaneko et al. 2003). Takai and Watanuki (2003) have reported that hydrogen trapping states are different in martensite steel and cold-drawn pearlite steel, which thereby varies the hydrogen embrittlement behavior of these steels. For titanium alloys, Yokoyama et al. have suggested that hydrogen absorption behaviors of alpha titanium, beta titanium, and alpha-beta titanium alloys are different in fluoride solutions (Yokoyama et al. 2004c, 2005b; Kaneko et al. 2003). The results indicate that the hydrogen embrittlement behavior of titanium alloys in fluoride solutions is dependent on the microstructure of the alloys. The influence of microstructure on the hydrogen embrittlement behavior of Ni-Ti alloys has been investigated with respect to the stress-induced martensite transformation (Yokoyama et al. 2003b, 2004d, 2009). There is a possibility that susceptibility to hydrogen embrittlement of Ni-Ti shape memory alloys is enhanced by interactions of hydrogen with dynamic processes such as martensite transformation and dislocation movement (Yokoyama et al. 2004d). Moreover, it has been proposed that the hydrogen embrittlement behavior of Ni-Ti superelastic alloy is closely related to the dynamic change of the hydrogen states that accompany martensite transformation (Yokoyama et al. 2009).

It is apparent that the hydrogen embrittlement of Ni-Ti alloys is closely related to the microstructure of the alloys. However, the influence of microstructure on the hydrogen embrittlement behavior of Ni-Ti alloys has been researched by cathodic hydrogen charging in 0.9 % NaCl aqueous solution. It has been demonstrated that the hydrogen state in Ni-Ti alloys changes with the hydrogen charging conditions such as the type of solution used for immersion tests (Yokoyama et al. 2003a, c, 2004b, 2012; Ogawa et al. 2005a, 2006). Therefore, the influence of microstructure on the hydrogen embrittlement behavior of Ni-Ti alloys under various hydrogen charging conditions should be clarified. In particular, fundamental data regarding the influence of microstructure on the hydrogen embrittlement behavior of Ni-Ti alloys in acidic fluoride solutions should be accumulated. This data could be a valuable contribution to improve the reliability and safety of Ni-Ti alloys as dental devices.

Therefore, the purpose of the present study is to investigate the hydrogen embrittlement behavior of Ni-Ti shape memory alloy with different microstructures in acidic fluoride solution. In the present study, three different microstructures of Ni-Ti shape memory alloy with different phases were employed; parent single phase, a mixture of parent and martensite phases, and martensite single phase were prepared by tensile preloading and unloading.

Methods

Commercial 0.50-mm diameter Ni-Ti (Ni, 55 mass%; Ti, balance) shape memory alloy wires were used. The specimens were cut into 50-mm lengths polished with 600-grit SiC papers and ultrasonically cleaned in acetone for 5 min. For the specimen with the microstructure of parent single phase, the critical stress of martensite transformation and the tensile strength were 102 and 1281 MPa, respectively. Three microstructures with different phases were prepared by tensile loading and unloading at room temperature (25 ± 2 °C). Specimen A has the parent single phase without loading. Specimen B (mixture of parent and martensite phases) was prepared by tensile loading to an intermediate strain range between the start and finish of martensite transformation and subsequent unloading. Specimen C (martensite single phase) was prepared by tensile loading to 500 MPa and subsequent unloading. The stress and strain histories for the preparation of each specimen are shown in Fig. 1. In addition, the microstructures of the specimens are shown in Fig. 2. In this study, we assume that specimen C is martensite single phase because a large portion of the microstructure of specimen C is martensite phase (Fig. 2c).

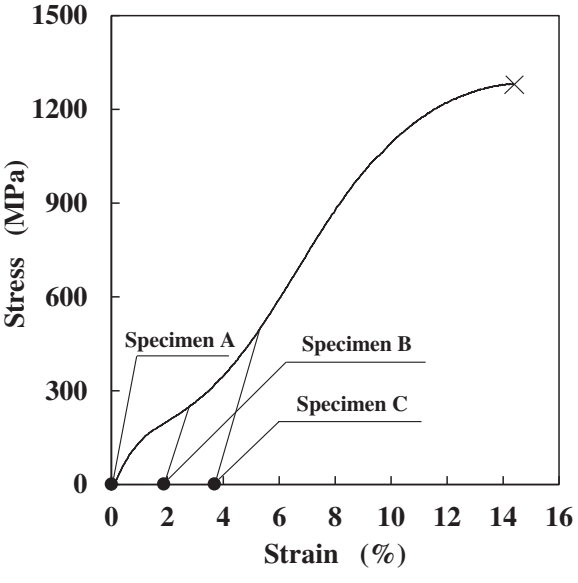

Fig. 1 Relationship between applied strain points of specimens *A*, *B*, and *C* and stress-strain curve of the Ni-Ti shape memory alloy

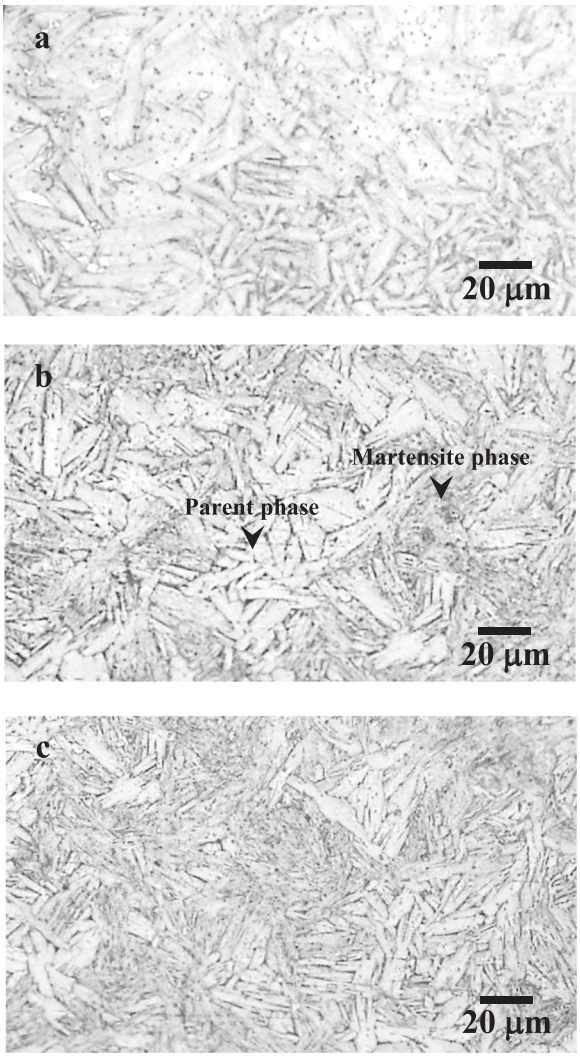

Fig. 2 Optical micrographs of **a** specimen A, **b** specimen B, and **c** specimen C

The specimens were immersed separately in 50 mL of 0.2 % acidulated phosphate fluoride (APF; 0.048 M NaF + 0.018 M H_3PO_4) solution with pH 5.0 at room temperature for various periods. After immersion, the specimens were ultrasonically cleaned in acetone for 5 min.

The mass loss of the immersed specimens with immersion time was measured using a microbalance. Tensile tests of the non-immersed and immersed specimens were conducted at room temperature and at a strain rate of 4.17×10^{-4} s^{-1} within a few minutes after removal of the specimens from the test solution. The gauge length of each specimen was 20 mm. Vickers microhardness tests of the non-immersed and immersed specimens were performed at room temperature from the surface to the center of the cross section of the wire at 0.05-mm intervals. Measurements were performed under an applied load of 0.98 N with an applied time of 15 s. Standard deviations of the mass loss, tensile strength, and Vickers hardness were calculated from the results obtained from five specimens.

The side surface and fracture surface of the tensile-tested specimens were observed using scanning electron microscopy (SEM). Hydrogen thermal desorption analysis (TDA) was performed in vacuum at 10^{-6} Pa using a quadrupole mass spectrometer. Sampling was conducted at 30-s intervals and at a constant heating rate of 100 °C h^{-1} up to 600 °C. TDA was started within 30 min after removal of the specimens from the test solution.

Results

Figure 3a–d shows typical stress-strain curves for the non-immersed and immersed specimens. The tensile strength for all the conditions of the specimens is represented as a function of the immersion time in Fig. 3e. As presented in Fig. 3b, the tensile strengths of the specimens were not significantly changed even after immersion for 2 h with respect to the non-immersed specimens. However, immersion time beyond 2 h led to considerable decrease in the tensile strengths for all the specimens. This is illustrated in Fig. 3c, d. For the immersion for 4 h, the tensile strength of specimen C was higher than that of specimens A and B. In the case of immersion for 6 h, the tensile strength of specimen B was lower than that of specimens A and C.

Figure 4 shows the corrosion rates in terms of mass loss of the immersed specimens. For all the specimens, the mass loss increased linearly with the immersion time. The mass loss of the immersed specimens was not dependent on the microstructure of the specimens for immersion times up to 4 h. However, after immersion for 6 h, the mass loss of the immersed specimens was in the order of C > B > A.

Figure 5 shows the side surfaces of the non-immersed and immersed specimens A. Scratches due to SiC paper polishing were observed in the non-immersed specimen (Fig. 5a, b). The scratches were still observed and partial corrosion was confirmed for the specimen immersed for 2 h (Fig. 5c, d). For the immersion for more than 4 h, general corrosion was observed and the scratches disappeared as a consequence (Fig. 5e–h). The morphologies of the side surfaces of the specimens B and C were similar to specimen A.

The total amounts of absorbed hydrogen in the immersed specimens are shown as a function of immersion time in Fig. 6. The amount of hydrogen absorbed during the immersion test was calculated by subtracting the amount of hydrogen desorbed from the non-immersed specimen from that desorbed from the immersed specimen. For all the specimens, the amount

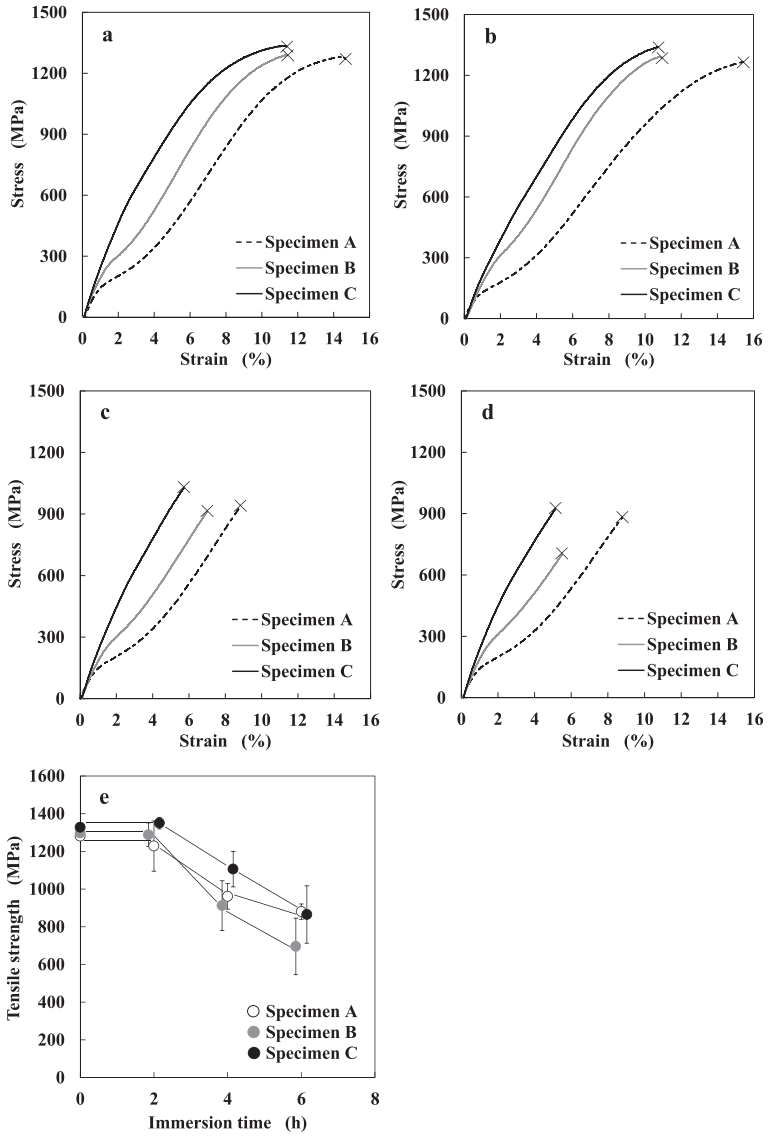

Fig. 3 Typical stress-strain curves of **a** non-immersed specimen and specimens immersed for **b** 2 h, **c** 4 h, and **d** 6 h in 0.2 % APF solution and **e** tensile strength of non-immersed and immersed specimens as a function of immersion time

of absorbed hydrogen increased linearly with the immersion time and was thus not dependent on the microstructure of the immersed specimens. The amounts of absorbed hydrogen in the specimens immersed for 2, 4, and 6 h were approximately 50, 130, and 240 mass ppm, respectively. Figure 7 shows the hydrogen thermal desorption curves from the immersed specimens. After immersion for 2 h, the hydrogen thermal desorption behavior varied with the microstructures of the immersed specimens (Fig. 7a). The hydrogen desorption peaks of specimens A, B, and C were approximately 500, 450, and 350 °C, respectively. In the case of the immersion for 4 and 6 h, the hydrogen desorption peaks appeared at around 450 °C for all the specimens (Fig. 7b, c). The differences in the shapes of the peak profile of the hydrogen thermal desorption curves could be primarily due to differences in the starting microstructures of the specimens.

Figure 8 shows SEM micrographs of fracture surfaces of the non-immersed and immersed specimen A. The fracture surface of the non-immersed specimen is ductile and characterized by cup-cone morphology (Fig. 8a). In addition, the fracture surface of the non-immersed specimen consists of primary and secondary dimples in the central part (Fig. 8b) and shear dimples in the outer part (Fig. 8c). No reduction in area was observed for the specimen immersed for 4 h

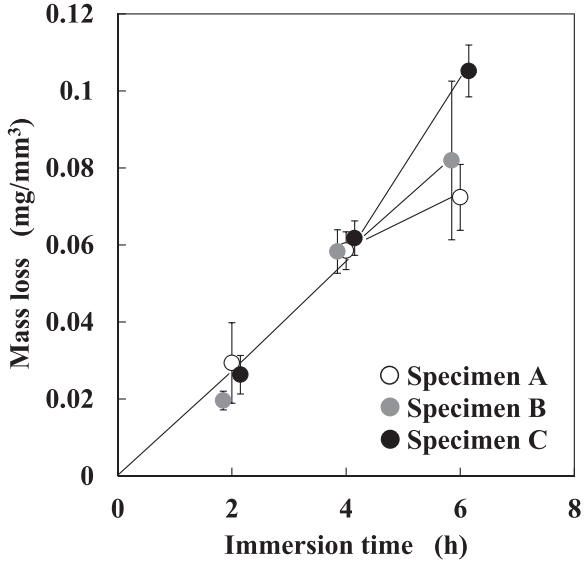

Fig. 4 Mass loss of immersed specimens as a function of immersion time

(Fig. 8d), and the central part of the fracture surface was composed of shallow dimples (Fig. 8e) while the outer part was flat (Fig. 8f). In the case of specimens B and C, the micrographs were similar to those for specimen A.

Figure 9 shows the Vickers microhardness along the diameter of the cross section of the immersed specimens. The hardness of the non-immersed specimens was approximately 260 throughout the specimens, irrespective of the specimen microstructure. In addition, the hardness distributions of the specimens immersed for 2 and 4 h were similar to those of the non-immersed specimens (Fig. 9a, b). After immersion for 6 h, an increase in hardness was confirmed at the peripheral parts of the cross-sectional area of the specimens (Fig. 9c). However, the hardness distributions of the immersed specimens were not significantly different for the different specimen microstructures.

Discussion

One noteworthy finding in the present study is that the hydrogen embrittlement behavior of the Ni-Ti shape memory alloy is different for the different microstructures of the alloy and changes with the immersion time in 0.2 % APF solution. Here, we discuss the hydrogen embrittlement behavior of the three specimens for each immersion time.

2-h immersion

As shown in Fig. 3, no significant degradation of tensile strength was confirmed for all of the specimens. This result indicates that hydrogen embrittlement of all the specimens does not occur after immersion for only 2 h. It has been reported that the tensile strength of Ni-Ti alloys is decreased when the amount of absorbed hydrogen exceeds at least 100 mass ppm (Yokoyama et al. 2003a, c, 2005a; Ogawa et al. 2005a). In this study, the amount of absorbed hydrogen after immersion for 2 h was approximately 50 mass ppm for all of the specimens. Thus, it appears that the critical amount of absorbed hydrogen for a loss of ductility is above at least 50 mass ppm, irrespective of the specimen microstructure. Here, it is well known that the hydrogen embrittlement behavior of metals is affected not only by the hydrogen content but also the hydrogen state, and the hydrogen state in metals is reflected by the hydrogen thermal desorption behavior. It has been reported that differences in the hydrogen state of the Ni-Ti alloys can change their hydrogen embrittlement behavior (Yokoyama et al. 2007a, 2009, 2012; Ogawa et al. 2005a; He et al. 2004; Gamaoun et al. 2011). As shown in Fig. 7a, the hydrogen thermal desorption behaviors of the immersed specimens were different according to the specimen microstructures, which implies that the hydrogen state in the immersed specimens can change with the specimen microstructure. It has been reported that hydrogen thermal desorption behavior of various metals is dependent on their microstructure (Takai and Watanuki 2003; Zhao et al. 2014; Ogawa et al. 2005a, b; Yokoyama et al. 2012; Kamoutsi et al. 2014), which is consistent with the results in the present study. However, hydrogen embrittlement did not occur in all the specimens immersed for 2 h; therefore, it is likely that the difference of the hydrogen state in the immersed specimens has negligible effect on the tensile strength of the specimens.

It has been demonstrated that the corrosion resistance of Ni-Ti alloys in solution environments is lower than that of titanium and titanium alloys (Shabalovskaya 2001; Ogawa et al. 2005a; Yokoyama et al. 2007b). In addition, it has been reported that the corrosion of Ni-Ti alloys in solution environments can degrade the mechanical properties of the alloys without hydrogen absorption (Yokoyama et al. 2004a, 2007b). For instance, the fracture of Ni-Ti superelastic alloy occurred due to localized corrosion under sustained tensile loading in a physiological saline solution containing hydrogen peroxide (Yokoyama et al. 2007b). The results of such previous studies indicate that corrosion of the specimens in 0.2 % APF solution could reduce the tensile strength of the specimens. Figure 5 shows that corrosion was observed in all of the specimens. However, no significant degradation of tensile strength was confirmed in all of the specimens; therefore, the effect of corrosion on the tensile strength of the immersed specimens is considered to be negligible.

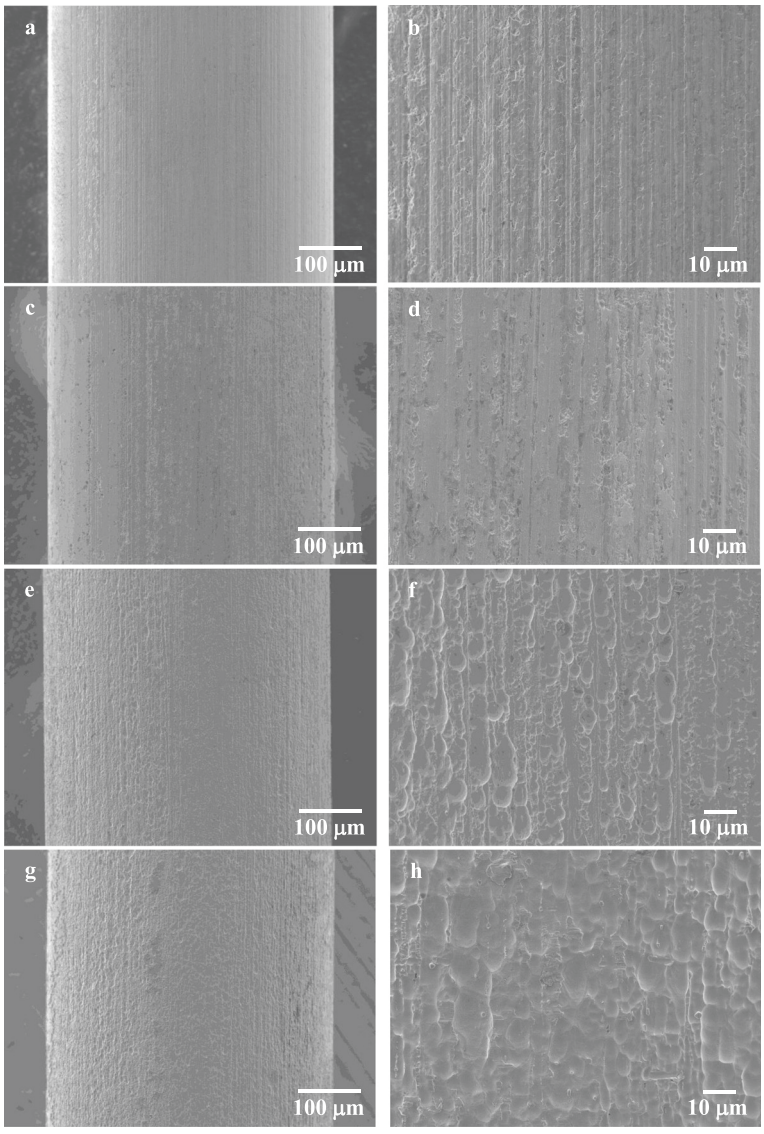

Fig. 5 SEM micrographs of typical side surfaces of **a** non-immersed specimen A and **b** magnified view of **a**, **c** specimen A immersed in 0.2 % APF solution for 2 h and **d** magnified view of **c**, **e** specimen A immersed in 0.2 % APF solution for 4 h and **f** magnified view of **e**, and **g** specimen A immersed in 0.2 % APF solution for 6 h and **h** magnified view of **g**

4-h immersion

As shown in Fig. 3, the tensile strength of the immersed specimens decreased, irrespective of the specimen microstructure. From the results of fracture surface observation, it is apparent that brittle fracture occurred in all of the specimens because no reduction area was observed and the outer part of the fracture surface was flat. Furthermore, the amount of absorbed hydrogen increased with the immersion time and reached approximately 130 mass ppm, irrespective of the specimen microstructure. These results indicate that the critical amount of absorbed hydrogen for a loss of ductility loss is probably not dependent on the specimen microstructure and is estimated to be approximately 100 mass ppm. Moreover, the estimated critical value (ca. 100 mass ppm) for loss of ductility is consistent with the previous studies (Yokoyama et al. 2003a, c, 2005a).

It should be noted that the tensile strength of specimen C was higher than that of specimens A and B after 4-h immersion in 0.2 % APF solution. This suggests that the susceptibility of specimen C to hydrogen embrittlement after 4-h immersion is lower than that of specimens A and B. The amount of absorbed hydrogen and the distribution of hydrogen were not dependent on the microstructure of the immersed specimens (Figs. 6 and 9); therefore, the susceptibility to hydrogen embrittlement cannot be explained by the amount of absorbed hydrogen or the distribution of hydrogen. With respect to

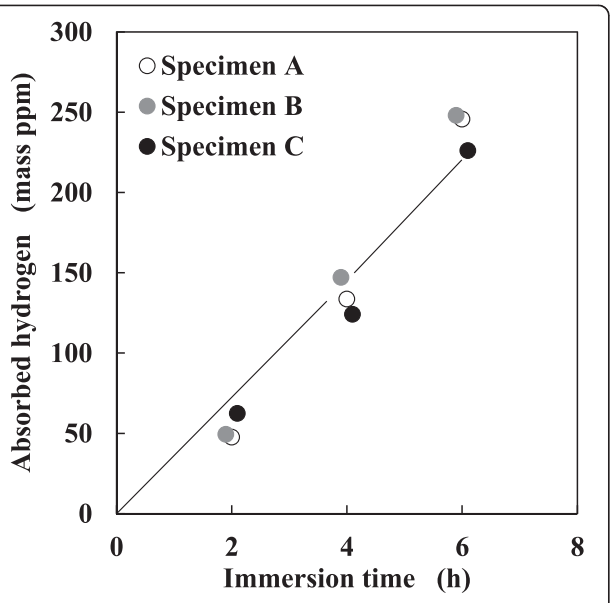

Fig. 6 Amounts of hydrogen absorbed in the immersed specimens as a function of immersion time

corrosion, the mass loss of the immersed specimens was also not dependent on the microstructure of the specimens. Moreover, the surface condition of the immersed specimens was not significantly different for the different specimen microstructures. Therefore, it appears that the effect of corrosion on the significant degradation of tensile strength for specimen B was negligible.

In the previous studies, it has been pointed out that the hydrogen embrittlement behavior of Ni-Ti alloys is strongly affected by the interaction of hydrogen with the dynamic phase transformation from the parent phase to the martensite phase (Yokoyama et al. 2004d, 2009). Thus, the susceptibility of Ni-Ti alloys with the parent phase to hydrogen embrittlement tends to be high. The microstructure of specimen C does not include the parent phase; therefore, the susceptibility to hydrogen embrittlement is lower than that of specimens A and B. In addition, the hydrogen thermal desorption behaviors of the immersed specimens were slightly different for the different specimen microstructures (Fig. 7b). The difference of the hydrogen state in the immersed specimens probably has an effect on the hydrogen embrittlement behavior of the specimens. Accordingly, the possibility that the tensile strength of the immersed specimens could be affected by the hydrogen state in each specimen cannot be ignored, although there were no significant differences in the hydrogen thermal desorption behaviors of the immersed specimens A, B, and C. The details of the hydrogen state in the immersed specimens are unclear and should therefore be investigated in the future.

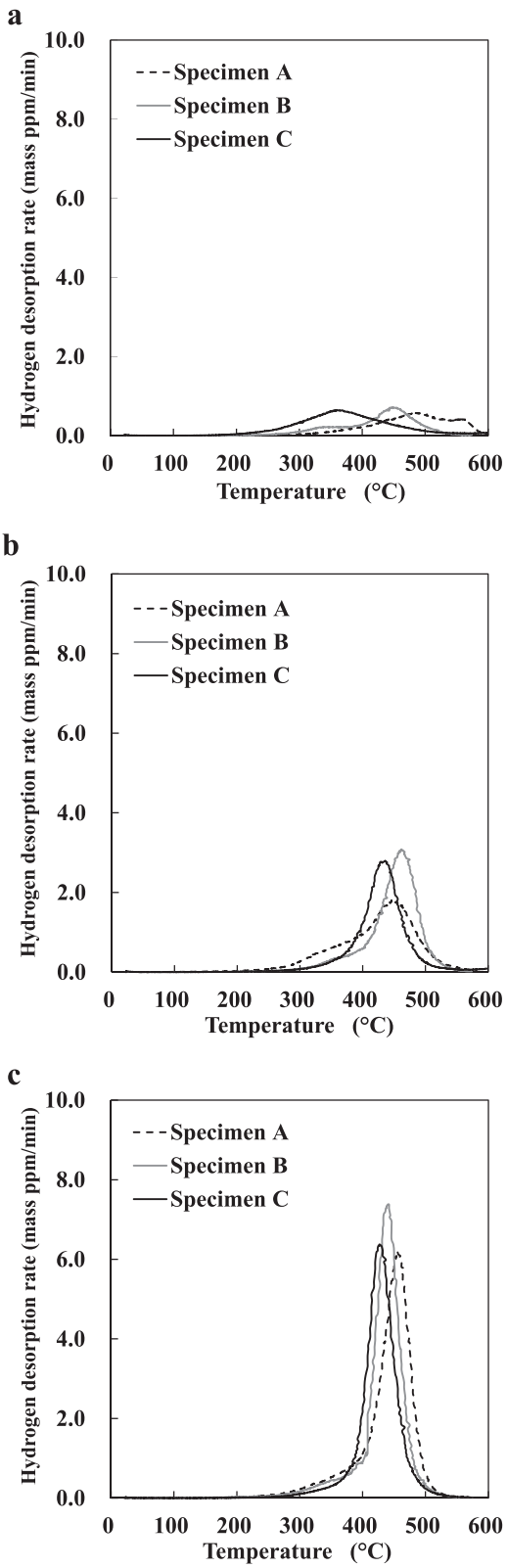

Fig. 7 Hydrogen thermal desorption curves for specimens immersed for **a** 2 h, **b** 4 h, and **c** 6 h in 0.2 % APF solution

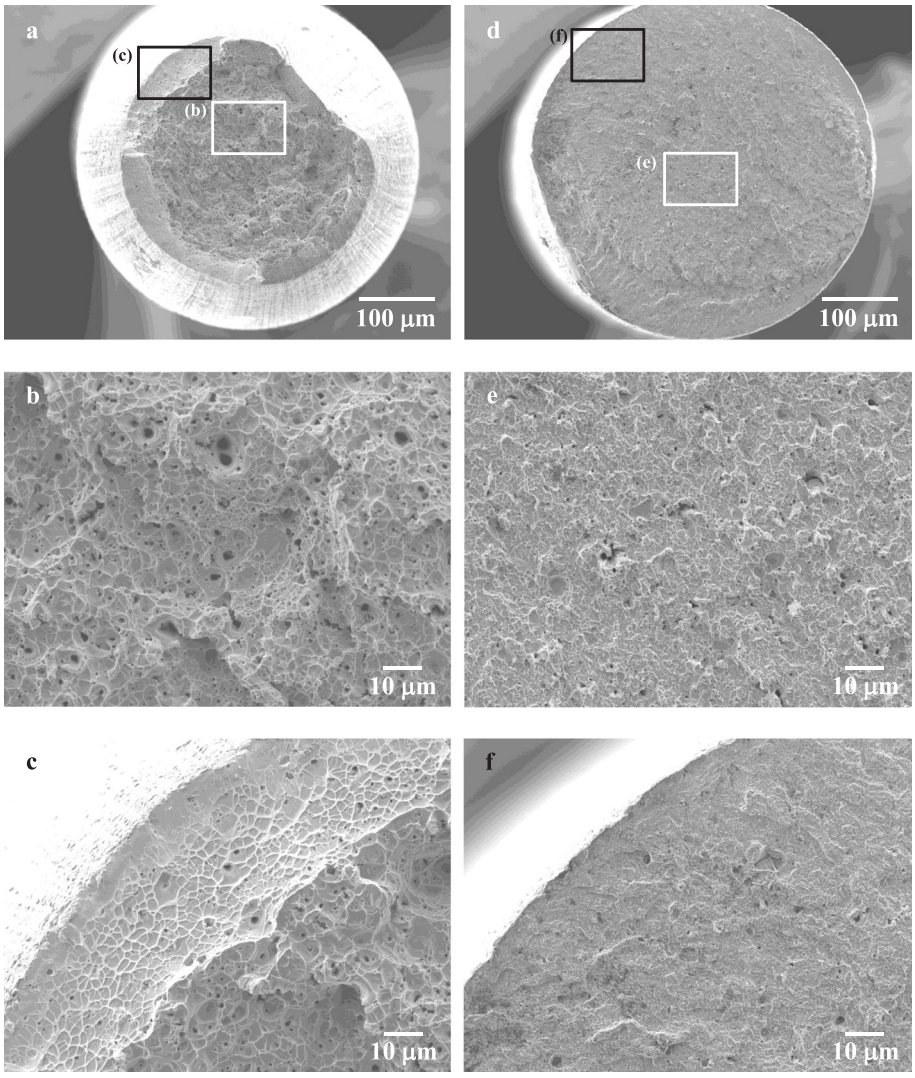

Fig. 8 SEM micrographs of typical fracture surfaces of **a** non-immersed specimen A and magnified views of **b** center and **c** outer parts in **a**, and **d** specimen A immersed in 0.2 % APF solution for 4 h and magnified views of **e** center and **f** outer parts in **d**

6-h immersion

Figure 3 shows that the tensile strength of specimen B is lower than that of specimens A and C, which indicates that specimen B is more susceptible to hydrogen embrittlement than specimens A and C during immersion for 6 h in 0.2 % APF solution. Consequently, the susceptibility to hydrogen embrittlement of each specimen was compared with the results for 4-h immersion. As shown in Figs. 6 and 9, the amount of absorbed hydrogen and the distribution of hydrogen were not dependent on the microstructure of the immersed specimens. Therefore, the significant degradation in the tensile strength of specimen B cannot be explained by the amount of absorbed hydrogen or the distribution of hydrogen. Furthermore, the tensile strengths of specimens A and C were almost the same, so that it is unlikely that the degradation of tensile strength for specimen B is only due to the interaction of hydrogen with the dynamic phase transformation from the parent phase to the martensite phase.

On the other hand, it should be noted that the mass loss of the immersed specimens was dependent on the specimen microstructure (Fig. 4). The mass loss of the immersed specimens was in the order of $C > B > A$; therefore, it appears that the susceptibility of the specimens to corrosion tends to be high for microstructures including the martensite. It has been reported that the corrosion of Ni-Ti alloys with microstructures including martensite phase is significant (Yokoyama et al. 2004a, 2007b), which is consistent with the results of the present study. Moreover, it has also been previously suggested that the acceleration of corrosion due to the presence of martensite phase in the microstructure of

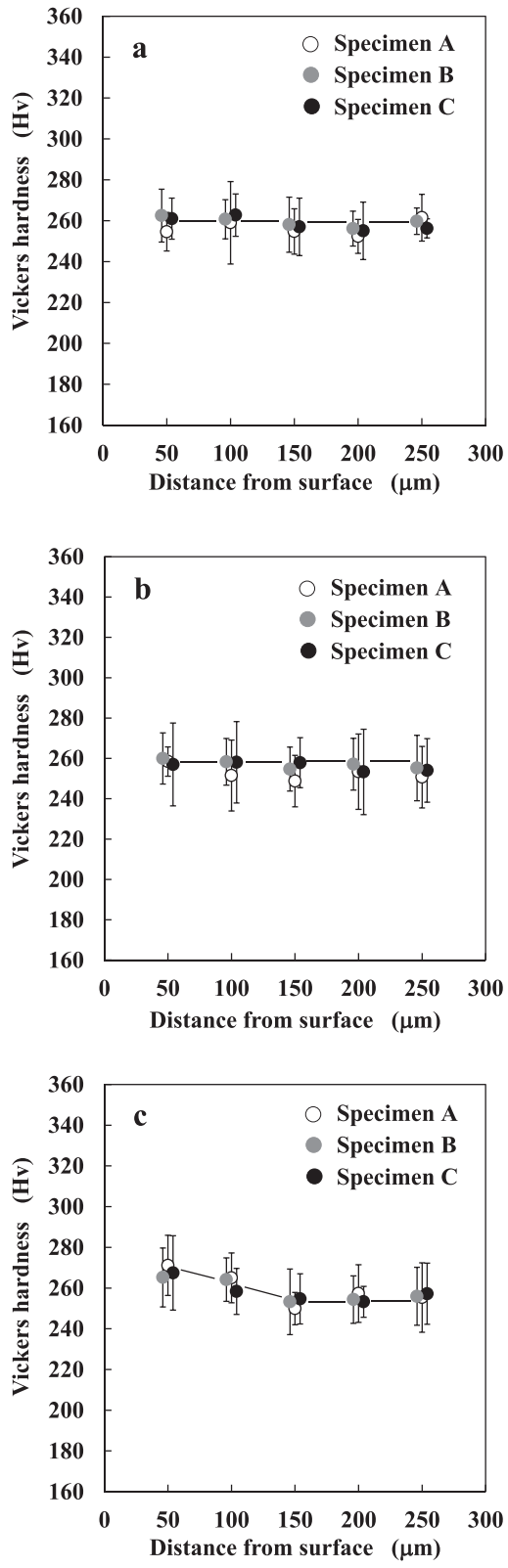

Fig. 9 Vickers microhardness of specimens immersed in 0.2 % APF solution for **a** 2 h, **b** 4 h, and **c** 6 h

Ni-Ti alloys can lead to shortening of the time to fracture of the alloys in sustained tensile loading tests (Yokoyama et al. 2004a, 2007b). Therefore, it is likely that the tensile strength of the immersed specimens is not only affected by hydrogen but also by the degree of corrosion.

From these results, the degradation in tensile strength due to hydrogen absorption for Ni-Ti shape memory alloys with microstructures including the parent phase may be significant, whereas the corrosion of alloys with microstructures including the martensite phase may be significant. Therefore, the significant degradation of tensile strength for specimen B is probably caused by a synergistic effect of hydrogen absorption and corrosion. In addition, the effect of corrosion on the tensile strength of specimen A was less than that of specimens B and C; therefore, the degradation of tensile strength for specimen A remained small when the immersion time was increased from 4 to 6 h. In the case of cathodic hydrogen charging without corrosion, the interaction of hydrogen with the dynamic phase transformation from the parent phase to the martensite phase is important for evaluation of the hydrogen embrittlement behavior of Ni-Ti shape memory alloys. We have revealed that the relationship between the characteristics of absorbed hydrogen, alloy microstructure, and corrosion behavior should be clarified to evaluate the hydrogen embrittlement behavior of alloys in corrosive environments.

Conclusions

The hydrogen embrittlement behavior of Ni-Ti shape memory alloy with different microstructures in acidic fluoride solution was examined, and the following results were obtained:

1. When the amount of absorbed hydrogen exceeds approximately 100 mass ppm, the tensile strength of the immersed specimens decreases, irrespective of the specimen microstructure.
2. The susceptibility to hydrogen embrittlement of the Ni-Ti shape memory alloy with a microstructure including the parent phase tends to be high when the degree of corrosion is not significantly different for the alloy microstructure.
3. The effect of corrosion on the tensile strength of Ni-Ti shape memory alloy is significant when the microstructure includes the martensite phase.

Competing interests
The authors declare that they have no competing interests.

Authors' contributions
TO drafted the manuscript. EY and TO carried out the experimental work. KM and JS guided the entire research work and made vital discussions. All authors read and approved the final manuscript.

Author details
[1]Department of Mechanical Engineering, National Institute of Technology, Kisarazu College, 2-11-1 Kiyomidai-higashi, Kisarazu-shi, Chiba 292-0041, Japan. [2]Department of Materials Science and Technology, Nagaoka University of Technology, 1603-1 Kamitomioka, Nagaoka-shi, Niigata 940-2188, Japan. [3]Faculty of Science and Engineering, Waseda University, 3-4-1 Okubo, Shinjuku-ku, Tokyo 169-8555, Japan. [4]Kagami Memorial Laboratory for Materials Science and Technology, Waseda University, 2-8-6, Nishiwaseda, Shinjuku-ku, Tokyo 169-0051, Japan.

Received: 19 May 2015 Accepted: 3 July 2015
Published online: 14 July 2015

References

Cheng, Y, Cai, W, & Zhao, LC. (2003). Effects of Cl^- ion concentration and pH on the corrosion properties of NiTi alloy in NaCl solution. *Journal of Materials Science Letters, 22*, 239–240.

Gamaoun, F, Ltaief, M, Bouraoui, T, & Zineb, TB. (2011). Effect of hydrogen on the tensile strength of aged Ni–Ti superelastic alloy. *Journal of Intelligent Material Systems and Structures, 22*, 2053–2059.

Gu, JL, Chang, KD, Fang, HS, & Bai, BZ. (2002). Delayed fracture properties of 1500 MPa bainite/martensite dual-phase high strength steel and its hydrogen traps. *ISIJ International, 42*, 1560–1564.

He, JY, Gao, KW, Su, YJ, Qiao, LJ, & Chu, WY. (2004). The role of hydride, martensite and atomic hydrogen in hydrogen-induced delayed fracture of TiNi alloy. *Materials Science and Engineering A, 364*, 333–338.

Huang, HH. (2007). Variation in surface topography of different NiTi orthodontic archwires in various commercial fluoride-containing environments. *Dental Materials, 23*, 24–33.

Huang, HH, Chiu, YH, Lee, TH, Wu, SC, Yang, HW, Su, KH, & Hsu, CC. (2003). Ion release from NiTi orthodontic wires in artificial saliva with various acidities. *Biomaterials, 24*, 2585–2592.

Kamoutsi, H, Haidemenopoulos, GN, Bontozoglou, V, Petroyiannis, PV, & Pantelakis, SG. (2014). Effect of prior deformation and heat treatment on the corrosion-induced hydrogen trapping in aluminium alloy 2024. *Corrosion Science, 80*, 139–142.

Kaneko, K, Yokoyama, K, Moriyama, K, Asaoka, K, Sakai, J, & Nagumo, M. (2003). Delayed fracture of beta titanium orthodontic wire in fluoride aqueous solutions. *Biomaterials, 24*, 2113–2120.

Lee, TH, Wang, CC, Huang, TK, Chen, LK, Chou, MY, & Huang, HH. (2009). Corrosion resistance of titanium-containing dental orthodontic wires in fluoride-containing artificial saliva. *Journal of Alloys and Compounds, 488*, 482–489.

Lekston, Z, Drugacz, J, & Morawiec, H. (2004). Application of superelastic NiTi wires for mandibular distraction. *Materials Science and Engineering A, 378*, 537–541.

Li, X, Wang, J, Han, EH, & Ke, W. (2007). Influence of fluoride and chloride on corrosion behavior of NiTi orthodontic wires. *Acta Biomaterialia, 3*, 807–815.

Mirjalili, M, Momeni, M, Ebrahimi, N, & Moayed, MH. (2013). Comparative study on corrosion behaviour of nitinol and stainless steel orthodontic wires in simulated saliva solution in presence of fluoride ions. *Materials Science and Engineering C, 33*, 2084–2093.

Nakasato, F, & Terasaki, F. (1975). Delayed fracture characteristics of tempered bainitic (BIII-type) and tempered martensitic steel. *Tetsu-to-Hagané, 61*, 856–868.

Nozue, A, Ikegaya, D, & Okubo, T. (1987). Hydrogen embrittlement behavior of structure controlled Ti-6Al-4V alloy. *Journal of the Japan Institute of Metals, 51*, 730–736.

Nozue, A, Endo, K, Tateishi, S, & Okubo, T. (1998). Hydrogen-induced cracking in titanium alloys. *Journal of the Japan Institute of Metals, 62*, 358–362.

Ogawa, T, Yokoyama, K, Asaoka, K, & Sakai, J. (2005a). Hydrogen embrittlement of Ni-Ti superelastic alloy in ethanol solution containing hydrochloric acid. *Materials Science and Engineering A, 393*, 239–246.

Ogawa, T, Yokoyama, K, Asaoka, K, & Sakai, J. (2005b). Distribution and thermal desorption behavior of hydrogen in titanium alloys immersed in acidic fluoride solutions. *Journal of Alloys and Compounds, 396*, 269–274.

Ogawa, T, Yokoyama, K, Asaoka, K, & Sakai, J. (2006). Effects of moisture and dissolved oxygen in methanol and ethanol solutions containing hydrochloric acid on hydrogen absorption and desorption behaviors of Ni–Ti superelastic alloy. *Materials Science and Engineering A, 422*, 218–226.

Oshida, Y, Sachdeva, R, Miyazaki, S, & Fukuyo, S. (1990). Biological and chemical evaluation of TiNi alloys. *Materials Science Forum, 56–58*, 705–710.

Rondelli, G. (1996). Corrosion resistance tests on NiTi shape memory alloy. *Biomaterials, 17*, 2003–2008.

Rondelli, G, & Vicentini, B. (1999). Localized corrosion behavior in simulated human body fluids of commercial Ni-Ti orthodontic wires. *Biomaterials, 20*, 785–792.

Schiff, N, Grosgogeat, B, Lissac, M, & Dalard, F. (2002). Influence of fluoride content and pH on the corrosion resistance of titanium and its alloys. *Biomaterials, 23*, 1995–2002.

Schiff, N, Grosgogeat, B, Lissac, M, & Dalard, F. (2004). Influence of fluoridated mouthwashes on corrosion resistance of orthodontics wires. *Biomaterials, 25*, 4535–4542.

Shabalovskaya, SA. (2001). Physicochemical and biological aspects of nitinol as a biomaterial. *International Materials Reviews, 46*, 233–250.

Takai, K, & Watanuki, R. (2003). Hydrogen in trapping states innocuous to environmental degradation of high-strength steels. *ISIJ International, 43*, 520–526.

Wang, J, Li, N, Rao, G, Han, EH, & Ke, W. (2007). Stress corrosion cracking of NiTi in artificial saliva. *Dental Materials, 23*, 133–137.

Yokoyama, K, Hamada, K, Moriyama, K, & Asaoka, K. (2001). Degradation and fracture of Ni-Ti superelastic wire in an oral cavity. *Biomaterials, 22*, 2257–2262.

Yokoyama, K, Kaneko, K, Moriyama, K, Asaoka, K, Sakai, J, & Nagumo, M. (2003a). Hydrogen embrittlement of Ni-Ti superelastic alloy in fluoride solution. *Journal of Biomedical Materials Research. Part A, 65*, 182–187.

Yokoyama, K, Watabe, S, Hamada, K, Sakai, J, Asaoka, K, & Nagumo, M. (2003b). Susceptibility to delayed fracture of Ni-Ti superelastic alloy. *Materials Science and Engineering A, 341*, 91–97.

Yokoyama, K, Ogawa, T, Asaoka, K, Sakai, J, & Nagumo, M. (2003c). Degradation of tensile strength of Ni-Ti superelastic alloy due to hydrogen absorption in methanol solution containing hydrochloric acid. *Materials Science and Engineering A, 360*, 153–159.

Yokoyama, K, Kaneko, K, Yabuta, E, Asaoka, K, & Sakai, J. (2004a). Fracture of nickel-titanium superelastic alloy in sodium hypochlorite solution. *Materials Science and Engineering A, 369*, 43–48.

Yokoyama, K, Kaneko, K, Moriyama, K, Asaoka, K, Sakai, J, & Nagumo, M. (2004b). Delayed fracture of Ni-Ti superelastic alloys in acidic and neutral fluoride solutions. *Journal of Biomedical Materials Research. Part A, 69*, 105–113.

Yokoyama, K, Kaneko, K, Miyamoto, Y, Asaoka, K, Sakai, J, & Nagumo, M. (2004c). Fracture associated with hydrogen absorption of sustained tensile-loaded titanium in acid and neutral fluoride solutions. *Journal of Biomedical Materials Research. Part A, 68*, 150–158.

Yokoyama, K, Eguchi, T, Asaoka, K, & Nagumo, M. (2004d). Effect of constituent phase of Ni-Ti shape memory alloy on susceptibility to hydrogen embrittlement. *Materials Science and Engineering A, 374*, 177–183.

Yokoyama, K, Kaneko, K, Ogawa, T, Moriyama, K, Asaoka, K, & Sakai, J. (2005a). Hydrogen embrittlement of work-hardened Ni-Ti alloy in fluoride solutions. *Biomaterials, 26*, 101–108.

Yokoyama, K, Ogawa, T, Asaoka, K, & Sakai, J. (2005b). Susceptibility to delayed fracture of alpha-beta titanium alloy in fluoride solutions. *Corrosion Science, 47*, 1778–1793.

Yokoyama, K, Ogawa, T, Takashima, K, Asaoka, K, & Sakai, J. (2007a). Hydrogen embrittlement of Ni-Ti superelastic alloy aged at room temperature after hydrogen charging. *Materials Science and Engineering A, 466*, 106–113.

Yokoyama, K, Ogawa, T, Fujita, A, Asaoka, K, & Sakai, J. (2007b). Fracture of Ni-Ti superelastic alloy under sustained tensile load in physiological saline solution containing hydrogen peroxide. *Journal of Biomedical Materials Research. Part A, 82*, 558–567.

Yokoyama, K, Tomita, M, & Sakai, J. (2009). Hydrogen embrittlement behavior induced by dynamic martensite transformation of Ni-Ti superelastic alloy. *Acta Materialia, 57*, 1875–1885.

Yokoyama, K, Nagaoka, A, & Sakai, J. (2012). Effects of the hydrogen absorption conditions on the hydrogen embrittlement behavior of Ni-Ti superelastic alloy. *ISIJ International, 52*, 255–262.

Zhao, J, Jiang, Z, & Lee, CS. (2014). Effects of tungsten on the hydrogen embrittlement behaviour of microalloyed steels. *Corrosion Science, 82*, 380–391.